3 Biotech (2019) 9:401
https://doi.org/10.1007/s13205-019-1912-4

ORIGINAL ARTICLE

A novel graphene oxide polymer gel platform for cardiac tissue engineering application

Li Zhao[1]

Received: 3 July 2019 / Accepted: 21 September 2019 / Published online: 18 October 2019

Abstract
In this study, we demonstrated a Reverse Thermal Gel (RTG), which is injectable and functionalized with GOs (GO–RTG) that changes at room temperature (24 °C) from a mixture to a three-dimensional (3D) matrix gel soon after approaching its body temperature (37 °C). We also presented investigational evidence, which represents that the system of 3D GO–RTG promotes MCs proliferation as well as alignment, supports in long-standing survival of MCs, and enhances the function of MCs when compared with typical 3D plain RTG system and 2D gelatin control groups. Thus, this system of injectable GO–RTG can be capable of using as a negligibly invasive device for engineering efforts of cardiac tissue.

Keywords Graphene · Cardiac · Tissue engineering

Introduction

Loss of myocardiocytes after Myocardial Infarction (MI) causes fibrosis and degradation of matrix that leads to the progression of cardiac injury (CI) (Konstam et al. 2011; Inamdar and Inamdar 2016; Cho et al. 2013). CI drives to an increased treat of mortality as well as a low quality of natural life expectancy (Braunwald 2013). Patients with last stage of CI were having heart transplantation as the only gold standard treatment, but then the accessibility of donors is the primary constraint (Li et al. 2015; Barr and Taylor 2015; Chin et al. 1999). With respect to limited availability of donors as well as partial regenerative capacity of cardiac muscle tissues, hereby creates a critical requirement for new treatment methodologies considering MI. Studies were concentrating on the improvement of biomaterials with the aim of restoring overall cardiovascular function as well as to support the site of infarct (Nelson et al. 2011; Johnson et al. 2014; Tous et al. 2011; Radisic and Christman 2013; Peña et al. 2018).

Hydrogels that were injectable can deliver a predominantly desiring methodology for treating MI. This can be possible with their capability of delivering in an insignificantly intrusive way, therefore reducing mechanical pressure on the cells while infusion as well as at the area of infarct, through this infarct can be provided with structural assistance too (Hasan et al. 2015; Janani and Sridhar Skylab 2014; Aguado et al. 2012). Moreover, these platforms contain 3D nature, which helps in enhanced mimicking of in vivo microenvironment better than the platforms containing 2D nature (Hirt et al. 2014). In particular, Reverse Thermal Gel (RTG) systems were more beneficial among all other injectable hydrogels, which is because they experience a transition of reversible solution-to-gelation (sol-to-gel) only via high-temperature stimuli (Park et al. 2012). This system is less toxic for tissues and encapsulated cells when compared with techniques that consider ultraviolet radiation for the purpose of crosslinking, whereas ultraviolet radiations can produce oxidative damage to the deoxyribonucleic acid (Rastogi et al. 2010).

Since natural heart tissues own distinctive electrophysiological conduct that is essential for the function of myocardiocytes (MCs) as well as for the transmission of electrical signals (Tandon et al. 2009). A perfect system of hydrogel would be conductive and assists in electrical signal transfer among the cells. Though the maximum of injectable hydrogels were electrically insulated, they hold excellent capability of using it in the heart tissue engineering (Shin et al.

✉ Li Zhao
lizhao1221@outlook.com

[1] Department of Cardiology, Third Affiliated Hospital of Qiqihar Medical University, NO 27, Taishun Street, Tiefeng District, Qiqihar City 161000, Heilongjiang Province, China

2013). In the process of enhancing the injectable hydrogels electrical properties, researchers have revised these injectable hydrogels by mixing with conducting NPs or by chemical conjugation, for example, gold nanoparticles (AuNPs) (Li et al. 2016; Shevach et al. 2014; Baranes et al. 2016; McCaffrey et al. 2014; Wu et al. 2006; He et al. 2016, Martín et al. 2015). AuNPs were extremely conductive non-hazardous biological structures (Wu et al. 2006) that present conducting properties to other unreactive cells.

In this study, we demonstrated a Reverse Thermal Gel (RTG), which is injectable and functionalized with GOs (GO–RTG) that changes at room temperature (24 °C) from a mixture to a three-dimensional (3D) matrix based on gel soon after approaching its body temperature (37 °C). Furthermore, we also presented investigational evidence, which represents that the system of 3D GO–RTG promotes MCs proliferation as well as alignment, supports in long-standing survival of MCs, and enhances the function of MCs when related with typical 3D plain RTG system and 2D gelatin control groups without GO.

Materials and methods

Materials

Hydroxy succinimide (NHS), Graphene oxide, *N*-(3-(dimethylamine) propyl)-*N*′-ethyl carbodiimide hydrochloride (EDC-HCl), hexamethylene diisocyanate (HDI), dichloromethane (DCM), anhydrous *N*,*N*-dimethylformamide (DMF), diethyl ether, trifluoroacetic acid (TFA), L-lysine monohydrochloride, graphene oxide (GO), and other solvents were obtained from Sigma-Aldrich, Shanghai.

Functionalization of GO

Graphene oxide functionalization with amino benzyl molecules with surface -NH_2 functionalities of 250 µmol g^{-1} was adjourned in 200 mL of 1 M NaOH (pH 8), followed by addition of succinic anhydride (20 mg). Later, the resulting mixture was allowed for stirring at 27 °C for about 16 h. The mixture was then filtered and washed with Milli Q water to obtain neutral pH followed by washing with diethyl ether as well as with methanol. The obtained powder was used for characterization studies.

Polymer synthesis

In brief, PSHU was prepared by treating N-BOC-serinol (1.147 g, 6 mmol), HDI (2.018 g, 12 mmol), and urea (0.36 g, 6 mmol) in anhydrous DMF (6 mL) at 90 °C for about 7 days under N_2 gas atmosphere. The corresponding suspension was then allowed for precipitation thrice with the help of anhydrous diethyl ether. Milli Q water was used for the removal of unreacted urea, and the polymer was lyophilized at − 45 °C for 48 h. The deportation of PSHU was performed with TFA/DCM (1:1, v/v) mixture (30 mL) and the corresponding reaction was carried out under room-temperature conditions for about 45 min, which was followed by three precipitations using diethyl ether. For preparation of PNIPAAm-COOH, NIPAAm (5 g, 800 mmol) was reacted with CVA (0.06 g, 4 mmol) at a temperature of 68 °C for about 3 h in anhydrous DMF (10 mL) under N_2 atmospheric conditions and the resulting mixture was undergone for boiled water (60 °C) precipitation. Milli Q water was used to dissolve the obtained polymer followed by dialysis for about 5 days.

The PNIPAAm-COOH conjugation onto PSHUNH_2 was carried out by following the below procedure. About 5 mL of anhydrous DMF was added with PNIPAAm-COOH (0.75 g, 1.21 mmol) along with five molar excess of EDC-HCl and NHS, allowed for dissolving under N_2 environment at room temperature for about 24 h. To the above solution, earlier prepared PSHU-NH_2 solution (1 mL, 0.125 gmL^{-1}) was mixed, allowed the reaction under room-temperature (24 °C) conditions for about 48 h at N_2 environment. The solution was then precipitated three times with diethyl ether. The resulting polymer was allowed for solubilizing in Milli Q water followed by dialysis for 5 days under room temperature and filtered. The purified solution was then lyophilized at − 45 °C for 2 days. For preparation of Poly(L-lysine), L-lysine (0.034 g, 5 mmol) along with five molar excess of EDC-HCl and NHS was dissolved in 5 mL of PBS buffer in a flask and stirred at a temperature of 4 °C for 15 min. Then, the earlier prepared solution of PSHU–PNIPAAm (10 mL, 0.1 g mL^{-1}) was dropwise added, later allowed for stirring for 48 h.

The polymer was then purified by following the process of dialysis for about 5 days, which later, filtered through filter paper followed by lyophilization at − 45 °C for about 2 days. For the graphene oxide conjugation, about 300 mg of GO-COOH was added to 15 mL of anhydrous DMF followed by ultra-sonication for about half an hour. To the above solution, 20 molar excess of EDC-HCl and NHS was mixed, later kept for stirring at room temperature for 15 m. The solution of RTG-lysine (5 mL, 0.1 g mL^{-1}) that was formed in anhydrous DMF was dropwise added, and the reaction was carried out at room temperature for 48 h. The mixture was then purified through centrifugation for five times for the removal of unreacted GO-COOH at 4 °C and dialyzed for 5 days following lyophilization for 2 days at − 45 °C. Later, L-Lysine (0.034 g, 15 mmol) was mixed to react with the remaining –COOH functionalities of GO.

L-Lysine in 5 mL of PBS buffer along with 5 molar excess of EDC-HCl and NHS was allowed for stirring at a temperature of 4 °C for about 15 m. Simultaneously, the COOH

functionalities of GO were conjugated to the RTG-lysine which were activated with five molar excess of EDC-HCl and NHS. The solution was then allowed for stirring at 4 °C for about 15 min. Later, activated L-lysine was dropwise added gradually to GO–RTG, and the subsequent reaction was carried out for 2 days under room-temperature conditions and dialyzed for about 5 days under room-temperature conditions followed by lyophilization at − 45 °C for 2 days.

Culture of neonatal rat ventricular myocytes (NRMs)

Neonatal rat ventricular myocytes (NRMs) were obtained from six rats of 1–3 day age. All the experiments related to animals were performed with the approval from institutional animal ethical committee and all experiments were performed according to their guidelines. Scissors were used for separating ventricles followed by their dissociation in bicarbonate and calcium free Hanks with Hepes buffer comprising pancreatine (1 mg/mL) and collagenase type 2 (500 mg mL^{-1}). Two sequential preplating steps were followed for enriching the myocardiocytes over nonmyocytes on 100 mm dishes in MEM supplemented with vitamin B12 (2 mg mL^{-1}) and bovine calf serum (5%) and then cultured. Later, the unattached cells were separated followed by culturing in 3D polymeric matrices and 2D gelatin-coated dishes and then undergone for various treatments and analyzed subsequently. All the above experiments were performed in triplicate on a minimum of three independent cell cultures.

Cell culture (3D in vitro)

Freshly obtained NRMs were used for in vitro 3D culture experiments by adding cells at a concentration of 9×10^4 along with polymer (150 µL), and then kept at 37 °C to obtain a gel. Later, warm cell culture medium of about 100 µL was supplementarily added on top.

Characterization

A JSM-6010LA scanning electron microscopy (SEM) instrument (JEOL, Tokyo, Japan) was used for morphological studies. Samples for SEM analysis were prepared by allowing the polymers (1% w/w) at 37 °C to form a gel. Later, gel was added with warm water on its top, followed by lyophilization at − 45 °C for about 2 days, which later studied under SEM. Philips EM 208 instrument was used for transmission electron microscopy (TEM) analysis, at an accelerating voltage of 100 kV. A TA Instruments Q500, was used for thermogravimetric analyses (TGA) using 60 mL min^{-1} of N_2 flow with sample weight from 0.7 to 1 mg. The prepared samples were allowed for heating for about 20 min to reach 100 °C followed by raising to 800 °C at a rate of 10 °C min^{-1}. Thermal Advantage v1.1A software was used for TGA interpretation. Furthermore, a Protek 6100 multimeter was used for recording resistance values. Samples for resistance recording were prepared by dissolving 400 µL of 1.5% (w/w) polymeric solution in deionized water which later was kept for formation of gel at 37 °C. All the gels were recorded for three times for resistance at various areas on gel. Milli Q water was used to evade external ions which affect the resistance of material. JPK NanoWizard 4a, atomic force microscope (AFM) was used to study the growth of MCs for about 21 days for their beating with the help of a Petri dish heater. For AFM analysis, the gel samples were kept for 5 min under room-temperature conditions to become solution from which the polymer is removed followed by washing with warm media. The MCs which traveled to the bottom of the plate were studied using AFM, through a triangular cantilever whose apex is glued with a gold colloidal probe, to obtain a force of 0.5 nN. Thermal noise method was followed for cantilever calibration. For every 2.5 s, recordings of beating height were done by allowing the constant cantilever force.

Immunocytochemistry

α-Sarcomeric actinin 1:100 (cardiac specific marker) was used for immunocytochemical staining after 8, 14, and 21 days of culture to examine the contractile gadget of MCs. Similarly, CD31 1:100 and vimentin 1:100 (a cytoskeleton marker) employed for staining of endothelial cells and fibroblasts, respectively. The secondary antibodies at 1:300 used were goat antirabbit antibody conjugated to TRITC, goat antichicken Cy5, and goat antimouse antibody conjugated to Alexa Fluor 488. To determine the junction gap area among MCs, Connexin 43 1:100 was examined after 21 days. The secondary antibody 1:300 used was goat antirabbit antibody conjugated to Alexa Fluor 594. Later, warm PBS 1X was used for washing 3D and 2D (control) cell cultures for two times followed by fixing in warm PBS containing 4% PFA for 15 min at 37 °C. Later, all the cells were treated for 1.5 h with warm 1% Triton X-100, and then blocked in warm 2% BSA for 45 min in PBS, followed by incubation for overnight with primary antibodies at 37 °C. Then, incubation of secondary antibodies was performed at 37 °C for 45 min. DAPI was used for staining cell nuclei followed by mounting in Vectashield. Cells were treated with Click-IT EdU 555 Imaging kit to know the incorporation of EdU, 12 h before analysis and DAPI staining was performed. A Zeiss LSM780 spectral, FLIM, 2P, SHG confocal instrument was used to take fluorescent microscopic images at four different locations in samples. Intracellular calcium signaling of MCs was recorded to examine the electrical activity of MCs mounting on the controls and 3D GO–RTG, after

21 days of culture. All the samples were added with cell-permeant fluo 4, AM followed by incubation for about 30 min for 3D polymeric groups and 15 min for 2D control groups. Before imaging, all the samples were washed thrice with warm media. A Zeiss LSM780 confocal microscope was used for recording calcium transients throughout impulsive beating of MCs for 20 s.

Statistical analysis

ANOVA software and Student's *t* test were performed for statistical examination. All the tests were carried out in triplicate and the value of $P \leq 0.05$ were taken as statistically accurate.

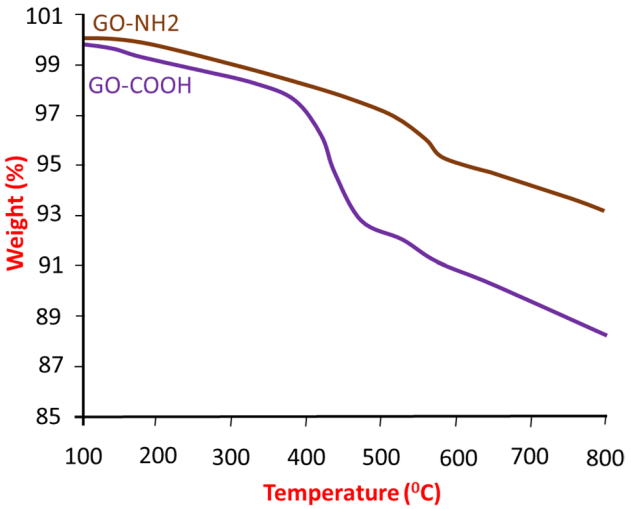

Fig. 1 TGA of GO-NH_2 and GO-COOH

Results and discussion

We prepared a conductive 3D RTG–GO platform, which supports the survival, proliferation and maturation of myocardiocytes using RTG-lysine. Due to the presence of a greater number of free primary amine groups in RTG-lysine polymer, GO can be easily functionalized with polymer. Hence, we prepared GO with -COOH functionalities by including amino benzyl groups to GO through the reaction of diazonium salt arylation. Then, succinic anhydride was used to include the -COOH functionalities. The introduction of COOH functionalities in the amino benzyl functionalized GO was studied using TGA analysis (Fig. 1). From the TGA results, it is found that a higher weight loss after reacting with succinic anhydride which followed by purification steps. Furthermore, Kaiser test exhibited an outstanding quantity of free amino functionalities (25 µmol/g), and the preliminary loading of -NH_2 functionalities was found to be 345 µmol/g, representing that -COOH functionalities were introduced into 92.7% of GO by weight. Furthermore, this greater percentage of COOH groups in GO is the perfect model to enable the conjugation with RTG-lysine.

The GO-COOH dispersed in DMF solvent was studied by TEM analysis. Figure 2 represents the TEM images which showed that the GO-COOH was dispersed well in DMF under room-temperature conditions after 30 min of sonication (shown in Fig. 2b inset), revealing its higher suitability for conjugations. It is found that the structure of GO-COOH is like a thin sheet, with transparent and silk like appearance, which seems to be highly stable under high-energy electron beam of TEM. Similar kind of TEM morphological images was already reported in literature (Maddinedi et al. 2014, 2015, 2018).

Scanning electron microscopy images showed the three-dimensional morphological analysis of both RTG-lysine as well as RTG–GO (shown in Fig. 3). SEM image of RTG-lysine exhibited highly porous configuration of 3D structure.

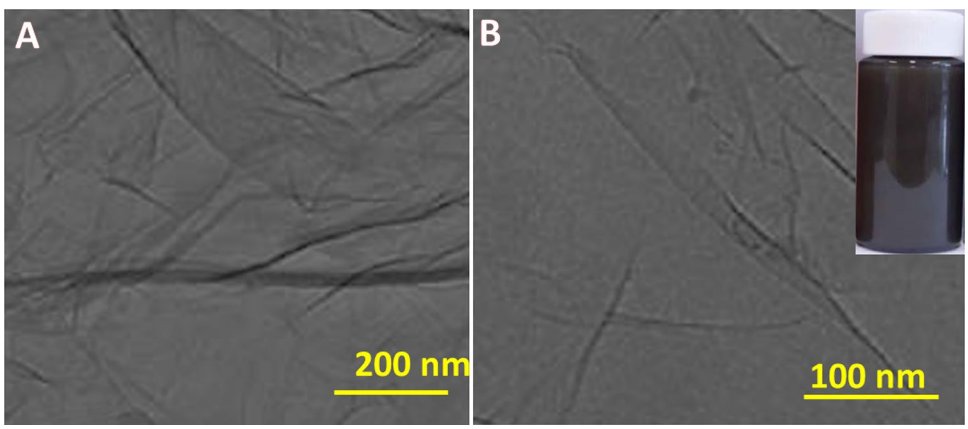

Fig. 2 TEM images of GO-COOH dispersion in DMF solvent

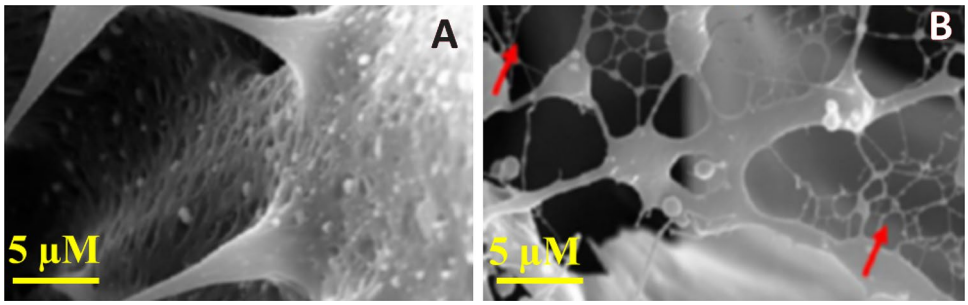

Fig. 3 SEM microscopic images of the RTG-lysine and RTG–GO. The red arrows in RTG–GO image represented the fibrous GOs mesh

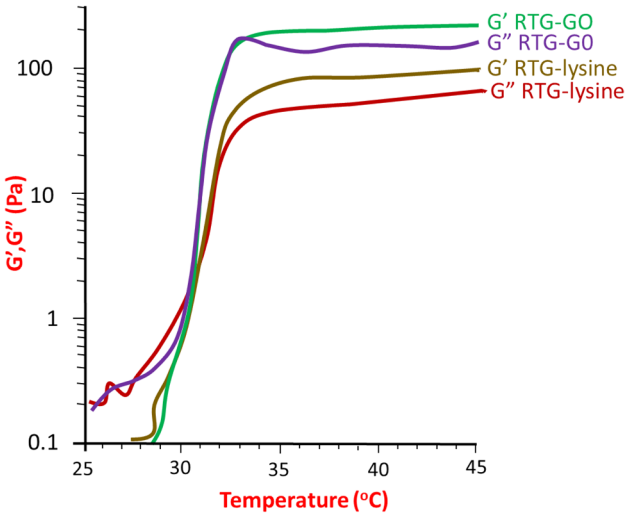

Fig. 4 Loss moduli and storage of both RTG-lysine and GO – RTG, and corresponding bottom lines represented the improved mechanical properties of RTG-lysine and aqueous solution of RTG–GO under the conditions of room temperature

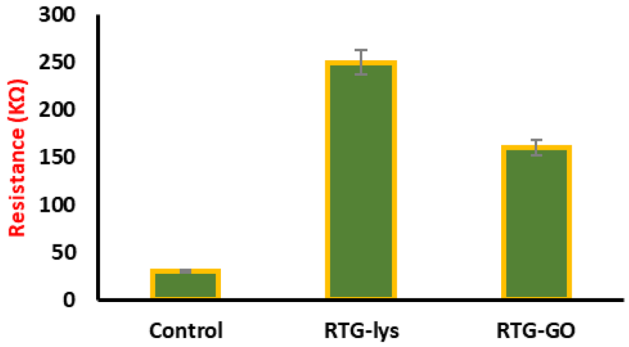

Fig. 5 Resistance measurements of RTG-lysine and RTG–GO

On the other hand, RTG–GO exhibited the presence of fibrous GOs mesh in SEM images, which may be advantageous for endorsing higher synchronized myocardiocytes contractions resulting in the electromechanical and electrophysiological host–cell coupling, which is an important field of future research examinations. However, similar kind of fibrous mesh network of carbon nanotube-based hydrogels was reported that are comparable to heart Purkinje fibers (Shin et al. 2013), which found in the inner walls of heart ventricles, functioning as a conductive system, generating coordinated contractions of left and right ventricles (Boyden et al. 2016; Brunello et al. 2014).

An oscillatory shear rheometric analysis was performed to know about the storage, sol–gel phase transition, as well as loss moduli (shown in Fig. 4). A temperature sweep was used to measure the sol-to-gel phase transition which was studied at ~ 31 °C (that is near body temperature) for gels with and without GO, which is ideal for in vivo studies. The obtained viscosity properties for RTG gels with and without GO exhibited that RTG–GO showed higher moduli i.e. $G' = 221 \pm 24.6$ Pa, $G'' = 146 \pm 21.6$ Pa when compared to RTG-lysine which is $G' = 82.0 \pm 4.2$ Pa, $G'' = 48.7 \pm 2.2$ Pa. Hence, it can be concluded that the chemical conjugation of GO advances the mechanical properties of RTG system, which further be helpful to improve the mechanical support to the wounded heart. Similarly, it was reported in the literature that alginate hydrogels were found to very good exercise capacity after they injected into the left-ventricular heart muscle (Anker et al. 2015).

Similarly, conducting resistance measurements were performed for electrical characterization of both the systems of RTG-lysine and GO–RTG (Fig. 5). It is found that RTG–GO showed less resistance at 37 °C when compared to RTG-lysine in nano-pure water (RTG–GO 144.3 KΩ ± 4.3; RTG-lysine: 236.8 KΩ ± 3; MWGO-COOH 24.3 KΩ ± 0.64), representing that GO-COOH and RTG–GO exhibited higher conductance than RTG-lysine.

Furthermore, the analysis of viscosity for both the systems of RTG-lysine and GO–RTG were carried out to know the use of prepared materials for cell delivery, and the comparison study was performed with cell culture media. Figure 6 exhibits that RTG-lysine and GO–RTG at about 1.5% showed a comparatively minimum viscosity that is advantageous for injecting polymer (RTG–GO: 13.4 + 2.5; RTG-lysine: 16.78 + 1.2; media: 21.9 + 0.8 mPa s).

The technique of immunocytochemistry was performed to investigate the phenotype as well as organization of the NRMs, which were cultured in 3D with the help of RTG

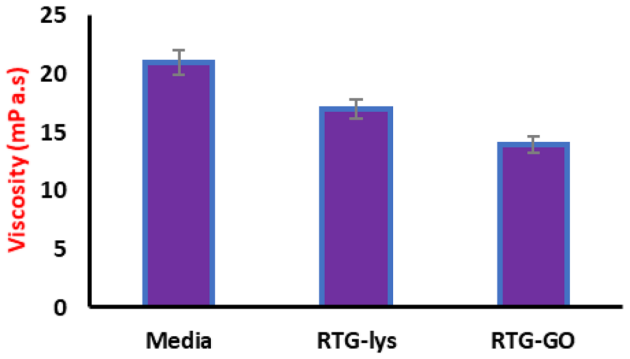

Fig. 6 Resistance measurements of RTG-lysine and RTG–GO

scaffolds. A protein associated with heart muscle contraction, α-sarcomeric actinin on staining was utilized as cardiovascular-specific indicator. A protein associated with cytoskeletal fibroblast, vimentin on staining was utilized to distinguish fibroblasts, which usually comprises around 10% population of the cell inside our NRMs' isolation procedure (Martinelli et al. 2013a, b). CD31 cells were utilized as an indicator for endothelial cells, which did not generally exist in the present protocol of MCs' development (Peña et al. 2016).

In contrast, no cells of positive CD31 were noticed in the culture as expected. However, through the technique of fluorescence microscopy, an obvious structure of cardiac sarcomere was revealed, which was showed by cross-striations in NRMs grownup in 3D by utilizing both the systems of RTG (Fig. 7). Despite the fact that a few of fibroblasts were also noticed in both the polymeric scaffolds, yet majority of the cells were noticed to be MCs as represented by their α-actinin-positive cardiovascular phenotype at all points of time (Fig. 8). Furthermore, α-actinin-positive cells were identified to be the majority portion of cells in the RTG systems when related with the cells cultured ion in the controls of 2D gelatin. On the other hand, when related with the polymeric systems, the quantity of fibroblasts increased significantly in the controls of 2D gelatin. In spite of the fact that initial culture proportion of fibroblast raised in the system of polymeric, evidently, the polymeric matrix stifled their long-standing proliferation capabilities; when related with the controls of 2D gelatin, these results were in accordance with one of the previously reported results (Peña et al. 2016). Furthermore, the microporous design of the three-dimensional reverse thermal gel scaffolds endorses elongation and cellular alignment of both fibroblasts as well as MCs, which can be favourable for both enhanced cell contractility as well as MCs' maturation.

On the other hand, while relating both the systems of RTG, it is noticed that the proportion of α-actinin-positive cells continued to be almost same at all points of time excluding day 7. On the 7th day, the number increased significantly in the system of carbon nanotubes–reverse thermal gel (GO–RTG).

While majority of the researchers were focusing on the investigation of MCs for restoration of cardiac tissues, it is also essential to study about endothelial cells as well as fibroblasts to restore the typical cardiac tissues. Critical functions like electrical stimuli propagation as well as electrical coupling with myocardiocytes were carried out by fibroblasts in the myocardium. To perform vascularization, endothelial cells are primarily essential as per previous reports (Vunjak-Novakovic et al. 2010). Despite the fact that endothelial cells were not been used in the current cultures, however, the purpose can be fulfilled by performing coculture of cardiac fibroblast and MCs in 3D which has an incredible capability of emerging as an artificial cardiovascular tissue.

Later, we evaluated the proliferation capability of 2D gelatin controls as well as NRMs cultured in both the RTG systems. Proliferation assay, 5-ethynyl-2′-deoxyuridine (EdU) was performed in absolute medium at 4, 3, and 2 days after seeding, to analyze the proliferation capabilities. The assay of EdU is a simple and extremely sensitive process that is used to label the freshly fabricated DNA of the cell proliferation. Moreover, when compared with rest of the traditional process like Phosphorylated-Histone H3 (pHH3) and BrdU52 (Martinelli et al. 2013a, b), which were used to identify cell division that is expressed only in cell proliferation, EdU has same rates and profiles of proliferating cells. Earlier, we have examined the influence of carbon nanotubes in the proliferation ability of MCs with the help of pHH3 and BrdU as indicators of cell proliferation (Martinelli et al. 2013a, b). We did not observe any kind of difference between both the indicators, in terms of proliferating cell rates. Thus, as EdU has similar proliferating cell rates than pHH3 and BrdU, EdU has been utilized to label the nuclei of cell proliferation, whereas to differentiate among fibroblast and cardiac cells, antibodies for α-sarcomeric vimentin and actinin were utilized, correspondingly. In contrast, all the systems of culture displayed incorporation of EdU at all the points of time (Fig. 9, red nuclei). On the 2nd day, depending on the quantity of positive EdU cells, we observed that the proliferating positive cells of α-sarcomeric actinin in the reverse thermal gel-lysine (39% ± 17.3) were significantly more than in the two-dimensional gelatin control groups (8.9% ± 2.1) or in the GO–RTG system (15.76% ± 1.27) (Fig. 10). On the other hand, the proportion of positive EdU NRMs in the system of GO–RTG raised to 23.3% ± 7 on the 3rd day. However, on the 3rd day, the number of proliferative NRMs reduced to 9.6% ± 4 on the system of RTG-lysine and the proportion of proliferative NRMs increasing on the gelatin control continued to be constant (6 ± 3). On the 4th day, the proportion of α-sarcomeric actinin and EdU positive cells reduced progressively according to time, and reached to their

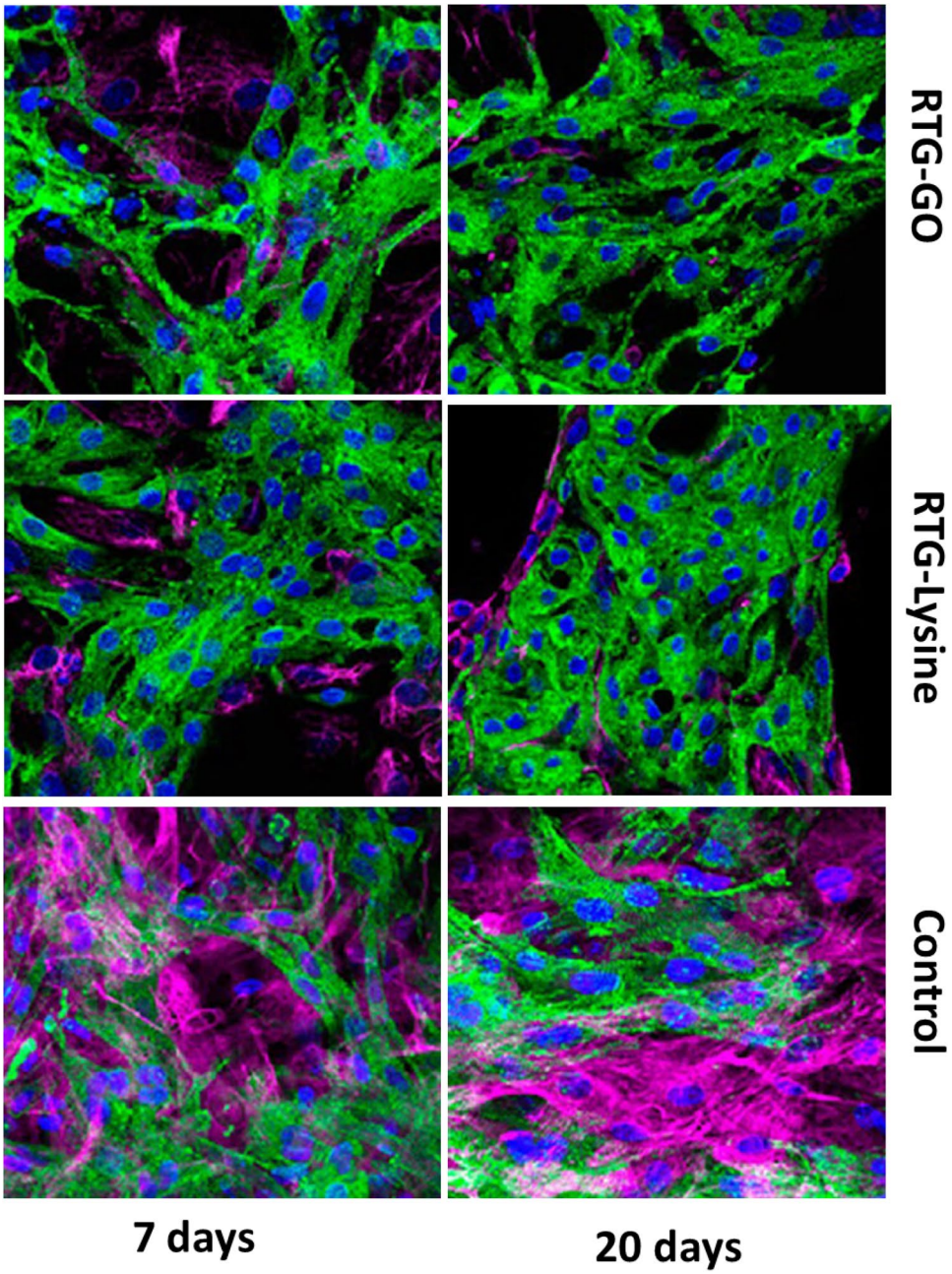

Fig. 7 Fluorescence staining images of fibroblasts and NRMs cultured in various substrates. α-DAPI (blue), vimentin (pink), as well as actinin (green)

lowest volumes of each systems (GO – RTG:15.8% ± 1.6, reverse thermal gel-lysine: 5% ± 1.3, 2D gelatin controls: 3.8% ± 1). As the restoring capabilities of MCs were not sufficient for total cardiac restoration after injury (Eulalio et al. 2012), also as the system of GO–RTG seems to enhance the proportion of cardiovascular cell division in the culture according to time, this process can be perfectly useful to endorse cell proliferation of MCs from the typical tissue as well as the transplanted MCs. On the other hand, when compared with the systems of RTG-lysine and GO – RTG, we observed an obvious increase of proliferating fibroblasts in the 2D gelatin controls on the 2nd day. No obvious change in the proliferating fibroblasts was noticed among the samples on the 3rd and 4th day.

As we know that one of the major prominent structural properties of heart is intercellular communication (Severs et al. 2004, 2008; Kostin et al. 2004), we examined the localizations as well as levels of gap intersections for Connexin 43 (C43) cells by immunostaining. Later, GO–RTG system was used to culture the cells for about 20 days followed by comparing with cells cultured in 3D RTG-lysine as well as 2D gelatin controls. Image J was used to quantify the portion of C43 in the positive cells of α-actinin. Figure 11 displays the illustrative images of NRMs stained for α-actinin

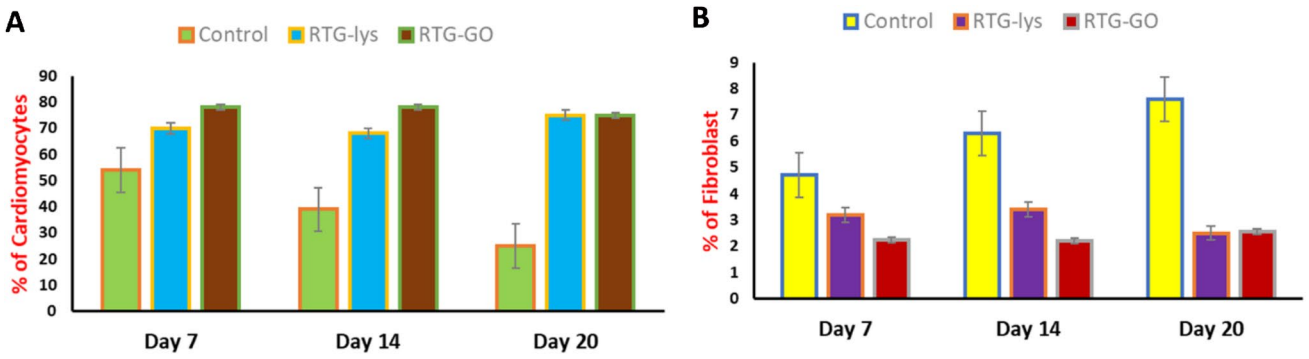

Fig. 8 Percentage quantification of growth of fibroblast and NRMs in RTG systems and gelatin control

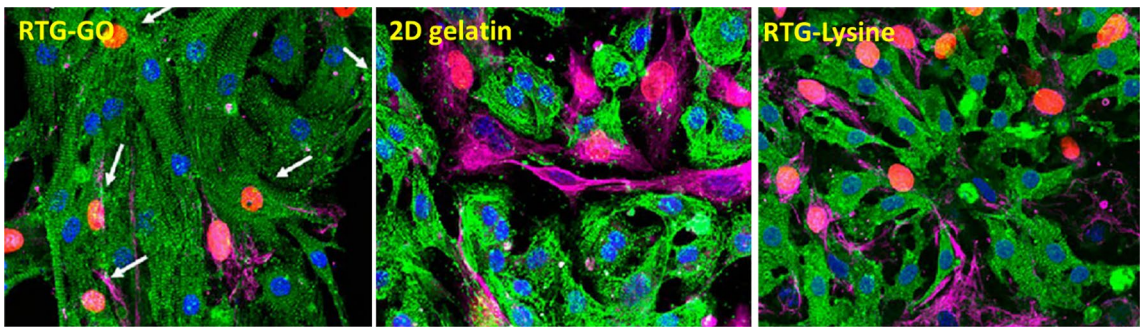

Fig. 9 Proliferation assay of fibroblasts and NRMs on various substrates

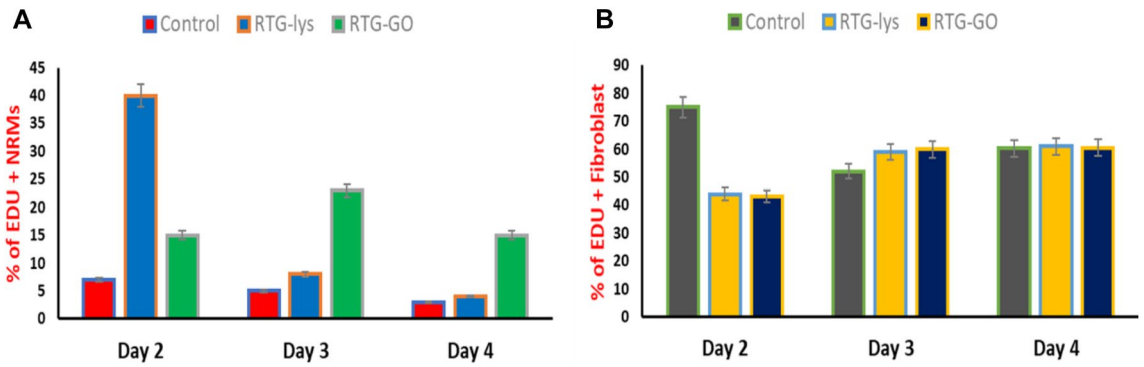

Fig. 10 Proliferation assay of fibroblasts and NRMs on various substrates on days 2, 3, and 4

(green) as well as C43 (red) post 20 days of culturing in the systems of RTG as well as two-dimensional gelatin control groups. When related with the systems of RTG-lysine (0.88 $\mu m^2 \pm 0.13$) and 2D gelatin controls (0.25 $\mu m^2 \pm 0.1$), we observed that the NRMs cultured in the system of GO–RTG were holding the greatest area of C43-positive (1.87 $\mu m^2 \pm 0.36$) (Fig. 12). As we already know that, NRMs that were cultured in the system of RTG-lysine were also holding a considerably higher area of C43-positive when related with the 2D gelatin vehicles. However, various investigational reports have demonstrated that the organization of C43 is essential for cellular impulse propagation as well as typical ventricular function in the healthy heart of human (Severs et al. 2004; Kostin et al. 2004). In contrast, the major mechanism directing to arrhythmias can be the modification of C43 organization (Martinelli et al. 2013a, b). As a result, the system of GO–RTG can stimulate a major organized portion of C43 expression that can be helpful in enhancing the

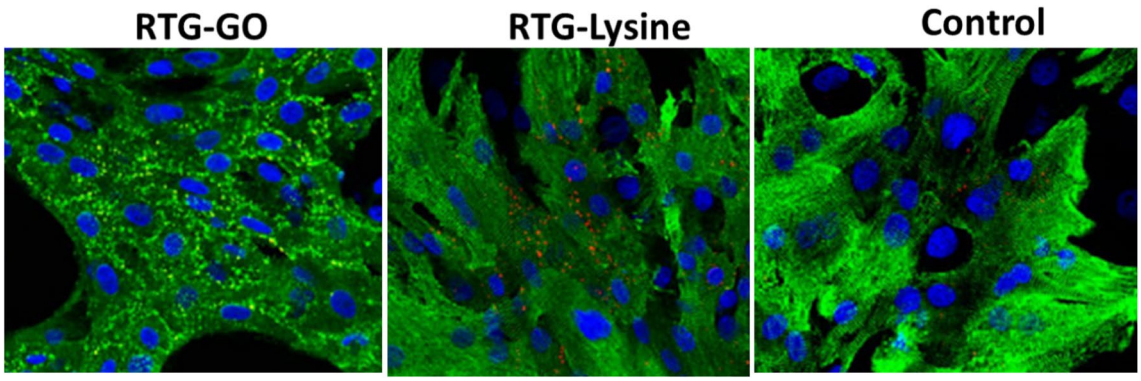

Fig. 11 Fluorescence images showing intercellular communication of NRMs after 20 days of culture growing on different substrates. DAPI (blue), sarcomeric α-actinin (green), and connexin 43 (red dots)

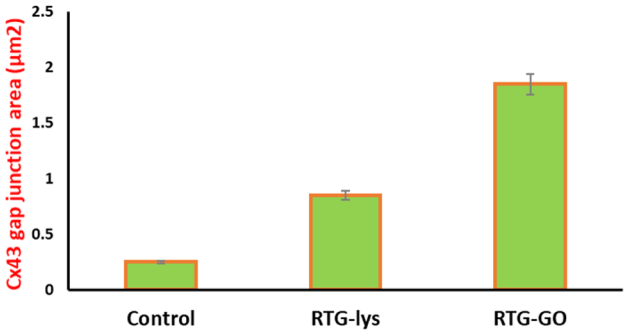

Fig. 12 Quantification of junction area of Cx43 gap for RTG–GO, RTG-lysine, and Control (2D gelatin)

integration as well as the function of transplanted MCs with the development and host of operational syncytia (Martinelli et al. 2013a, b).

One of the earlier reports stated that systematized instinctive intracellular calcium fluctuations were interlinked with MCs cell function as well as maturation (Martinelli et al. 2013a, b). To examine the cellular heart functions, we picturized the instinctive calcium oscillations to evaluate NRMs' electrical movement post-culturing for 20 days (data not shown). When related with the cells cultured in 2D gelatin controls, we noticed that NRMs cultured in 3D RTG-lysine, 3D GO–RTG contains significantly more recurrent calcium transients. We also observed that when compared to system of RTG-lysine, NRMs cultured in the system of 3D GO–RTG significantly holds greater similar calcium transients (synchronized oscillations with homogeneous frequency). Furthermore, 83 and 94% of the analyzed overall cells (35) in the RTG-lysine system as well as gelatin controls, respectively, present a similar calcium oscillation with 95% of the analyzed overall cells (35) in the system of GO–RTG. Thus, these responses backup the proposal of combining a 3D nature ecosystem along with the existence of carbon nanotubes, which could enhance the MCs intracellular function as well as communication towards a greater matured cardiac composition.

Atomic force microscopy was performed to measure the spontaneous oscillations of NRMs cultured in the 2D gelatin control group as well as RTG systems on the 20th day. When compared with other technologies, atomic force microscopy can be utilized to measure the refraction of a bendable cantilever at the time of interaction with the bottom of the cell, which helps to analyze the biomechanical characteristics of the cells Lanzicher et al. (2015a, b). Atomic force microscopy was used in few of the earlier investigations to effectively record the modified nuclear mechanical characteristics of MCs with the help of cardiomyopathy mutation (LMNA D192G) (Lanzicher et al. 2015a, b). Atomic force microscopy could also be utilized to record the elevation of instinctive oscillations of MCs. In the current examination, NRMs were cultured for 20 days in the system of RTG, and then, the cells were retrieved for the examination by utilizing the flexible characteristic of the gels. The temperature was reduced to 25 °C, which made the RTGs convert to mixture, by which the MCs transferred to the plate surface, and finally, they were studied. The activity of beating of NRMs was recorded as heights in the reflection of the cantilever, which provides facts regarding the height and frequency recorded during the phases of depolarization and polarization. The MCs' activity of beating, cultured in various conditions, is represented in Fig. 13. These responses achieved with the atomic force microscopy were in accordance with those achieved with the analysis of calcium transient. Consequently, this verifies the significance of a 3D environment to deliver intracellular communication as well as cell support. On the other hand, NRMs that are cultured in the 3D GO–RTG displayed greater contraction during beating (Fig. 13), signifying that the environment of 3D GO–RTG backs a higher effective contraction of MCs.

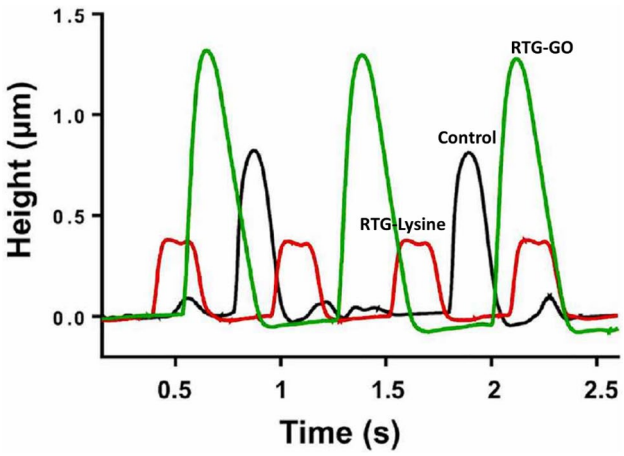

Fig. 13 AFM analysis of spontaneous beating of NRMs cultured for 20 days in various substrates

These responses recommend that the 3D GO–RTG system could be better than the system of RTG-lysine, while the 2D gelatin controls is being beneficial for durable cardiovascular cell growth (i.e., up to 20 days), function, and proliferation, demonstrating that the biological conjugation of carbon nanotubes to the system of RTG-lysine enhances the system's biocompatibility, which finally makes the GO–RTG system as a favourable mechanism for the applications of in vivo.

There is a possibility of carbon nanotubes to inhibit nutritious from an exterior source and further play as transporters supporting in a greater direct cells adsorption of proteins. Moreover, since the carbon nanotubes were extremely conducting materials of electricity (Bosi et al. 2013), quite a few studies represented that carbon nanotubes enhance intracellular interaction (Shin et al. 2013; Martinelli et al. 2013a, b) endorsing MCs maturing. In contrast, the accurate impact of carbon nanotubes on MCs was not yet revealed completely and was highly considered to investigate further. However, the microporous framework of 3D RTG scaffolds endorses a higher structured cellular arrangement impersonating the cardiovascular tissue as reported earlier (Peña et al. 2016). Thus, carbon nanotubes and 3D RTG function improve the survival of MCs, function, and proliferation development. On the other hand, the utilization of RTG–GO environment as a cell distribution system in an in vivo mechanism as well as the knowledge of carbon nanotubes impact on MCs proliferation, maturation, and their survival were required to be examined further.

Conclusions

To conclude, we have prepared a system of an injectable conductive atmosphere, specifying cues of both electrophysiological as well as topographical for natural MCs. This developed system improves long-standing survival of MCs along with a better-aligned organization of cell, as well as enhanced cellular maturation and function. Moreover, on combining GO with 3D system helps MCs proliferation and decreases long-lasting proliferation of fibroblast. As we know the fact that GOs were always having an issue of safety, here in this study, we exhibited that the GOs chemical conjugation with the system of RTG-lysine enhances the GOs proliferation, survival, function, as well as alignment, validating that the polymer of GO–RTG is no more cytotoxic in vitro. Finally, as per our knowledge, this system of GO–RTG with low viscosity that switches to a three-dimensional matrix depending on temperature variation has not only an incredible capability for negligibly invasive methods to restore injured cardiac tissue, but can also be potentially utilized as a three-dimensional scaffold for the investigations of in vitro.

Funding This research was supported by Heilongjiang Qigihar Science and Technology Department (CN) (Grant SFZD-2017028).

References

Aguado BA, Mulyasasmita W, Su J, Lampe KJ, Heilshorn SC (2012) Improving viability of stem cells during syringe needle flow through the design of hydrogel cell carriers. Tissue Eng Part A 18(7–8):1806–1815

Anker SD, Coats AJS, Cristian G, Dragomir D, Pusineri E, Piredda M, Bettari L, Dowling R, Volterrani M, Kirwan BA, Filippatos G, Mas JL, Danchin N, Solomon SD, Lee RJ, Ahmann F, Hinson A, Sabbah HN, Mann DL (2015) A prospective comparison of alginate-hydrogel with standard medical therapy to determine impact on functional capacity and clinical outcomes in patients with advanced heart failure (AUGMENT-HF Trial). Eur Heart J 36(34):2297–2309

Baranes K, Shevach M, Shefi O, Dvir T (2016) Gold nanoparticle-decorated scaffolds promote neuronal differentiation and maturation. Nano Lett 16(5):2916–2920

Barr ML, Taylor DO (2015) Changes in donor heart allocation in the United States without fundamental changes in the system: rearranging deck chairs and elephants in the room. Am J Transplan 15(1):7–9

Bosi S, Fabbro A, Ballerini L, Prato M (2013) Carbon nanotubes: a promise for nerve tissue engineering? Nanotechnol Rev 2(1):47–57

Boyden PA, Dun W, Robinson RB (2016) Cardiac purkinje fibers and arrhythmias; the GK moe award lecture 2015. Hear Rhythm 13(5):1172–1181

Braunwald E (2013) Heart failure. JACC Hear Fail 1(1):1–20

Brunello L, Knollmann BC, Janssen PML, Gyorke S (2014) Relative contribution of purkinje fibers to $CA^{(2+)}$—dependent arrhythmias in a murine model of CPVT. Biophys J 106(2):112A

Chin C, Miller J, Robbins R, Reitz B, Bernstein D (1999) The use of advanced-age donor hearts adversely affects survival in pediatric heart transplantation. Pediatr Transpl 3(4):309–314

Cho E, Kim M, Ko YS, Lee HY, Song M, Kim MG, Kim HK, Cho WY, Jo SK (2013) Role of inflammation in the pathogenesis of cardiorenal syndrome in a rat myocardial infarction model. Nephrol Dial Transplant 28(11):2766–2778

Eulalio A, Mano M, Dal Ferro M, Zentilin L, Sinagra G, Zacchigna S, Giacca M (2012) Functional screening identifies miRNAs inducing cardiac regeneration. Nature 492(7429):376–381

Hasan A, Khattab A, Islam MA, Hweij KA, Zeitouny J, Waters R, Sayegh M, Hossain MM, Paul A (2015) Injectable hydrogels for cardiac tissue repair after myocardial infarction. Adv Sci 2(11):1–18

He L, Dragavon J, Cho S, Mao C, Yildirim A, Ma K, Chattaraj R, Goodwin AP, Park W, Cha JN (2016) Self-assembled gold nanostar-NaYF4:Yb/Er clusters for multimodal imaging, photothermal and photodynamic therapy. J Mater Chem B 4(25):4455–4461

Hirt MN, Hansen A, Eschenhagen T (2014) Cardiac tissue engineering: state of the art. Circ Res 114(2):354–367

Inamdar A, Inamdar A (2016) Heart failure: diagnosis, management and utilization. J Clin Med 5(7):62

Janani A, Sridhar Skylab R (2014) Injectable hydrogel for cardiac tissue engineering. Int J ChemTech Res 6(3):2233–2236

Johnson TD, Braden RL, Christman KL (2014) Injectable ECM scaffolds for cardiac repair. Methods Mol Biol 1181(6):109–120

Konstam MA, Kramer DG, Patel AR, Maron MS, Udelson JE (2011) Left ventricular remodeling in heart failure: current concepts in clinical significance and assessment. JACC Cardiovasc Imaging 4(1):98–108

Kostin S, Dammer S, Hein S, Klovekorn WP, Bauer EP, Schaper J (2004) Connexin 43 expression and distribution in compensated and decompensated cardiac hypertrophy in patients with aortic stenosis. Cardiovasc Res 62(2):426–436

Lanzicher T, Martinelli V, Long CS, Del Favero G, Puzzi L, Borelli M, Mestroni L, Taylor MRG, Sbaizero O (2015a) AFM single-cell force spectroscopy links altered nuclear and cytoskeletal mechanics to defective cell adhesion in cardiac myocytes with a nuclear lamin mutation. Nucleus 6(5):394–407

Lanzicher T, Martinelli V, Puzzi L, Del Favero G, Long CS, Mestroni L, Taylor MRG, Sbaizero O, Barbara C (2015b) The cardiomyopathy lamin A/C D192G mutation disrupts whole-cell biomechanics in cardiomyocytes as measured by atomic force microscopy loading-unloading curve analysis. Sci Rep 5(1):1–14

Li S, Loganathan S, Korkmaz S, Radovits T, Hegedus P, Zhou Y, Karck M, Szabó G (2015) Transplantation of donor hearts after circulatory or brain death in a rat model. J Surg Res 195(1):315–324

Li Y, Shi X, Tian L, Sun H, Wu Y, Li X, Li J, Wei Y, Han X, Zhang J, Jia X, Bai R, Jing L, Ding P, Liu H, Han D (2016) AuNP–collagen matrix with localized stiffness for cardiac-tissue engineering: enhancing the assembly of intercalated discs by B1-integrin-mediated signaling. Adv Mater 28(46):10230–10235

Maddinedi SB, Mandal BK, Vankayala R, Kalluru P, Tammina SK, Kiran Kumar HA (2014) Casein mediated green synthesis and decoration of reduced graphene oxide. Spectrochim Acta Part A 126:227–231

Maddinedi SB, Mandal BK, Vankayala R, Kalluru P, Pamanji SR (2015) Bio-inspired reduced graphene oxide nanosheets using *Terminalia chebula* seeds extract. Spectrochim Acta Part A 145:117–124

Maddinedi SB, Sonamuthu J, Yildiz SS, Han G, Cai Y, Gao J, Ni Q, Yao Y (2018) Silk sericin induced fabrication of reduced graphene oxide and its in vitro cytotoxicity, photothermal evaluation. J Photochem Photobiol, B 186:189–196

Martín C, Merino S, Prato M, Vázquez E, Kostarelos K (2015) Nanocomposite hydrogels: 3D polymer-nanoparticle synergies for on-demand drug delivery. ACS Nano 9(5):4686–4697

Martinelli V, Cellot G, Fabbro A, Bosi S, Mestroni L, Ballerini L (2013a) Improving cardiac myocytes performance by carbon nanotubes platforms. Front Physiol 4:1–6

Martinelli V, Cellot G, Toma FM, Long CS, Caldwell JH, Zentilin L, Giacca M, Turco A, Prato M, Ballerini L, Mestroni L (2013b) Carbon nanotubes instruct physiological growth and functionally mature syncytia: nongenetic engineering of cardiac myocytes. ACS Nano 7(7):5746–5756

McCaffrey R, Long H, Jin Y, Sanders A, Park W, Zhang W (2014) Template synthesis of gold nanoparticles with an organic molecular cage. J Am Chem Soc 136(5):1782–1785

Nelson DM, Ma Z, Fujimoto KL, Hashizume R, Wagner WR (2011) Intra-myocardial biomaterial injection therapy in the treatment of heart failure: materials, outcomes and challenges. Acta Biomater 7(1):1–15

Park MH, Joo MK, Choi BG, Jeong B (2012) Biodegradable thermogels. Acc Chem Res 45(3):424–433

Peña B, Martinelli V, Jeong M, Bosi S, Lapasin R, Taylor MRG, Long CS, Shandas R, Park D, Mestroni L (2016) Biomimetic polymers for cardiac tissue engineering. Biomacromol 17(5):1593–1601

Peña B, Laughter M, Jett S, Rowland TJ, Taylor MRG, Mestroni L, Park D (2018) Injectable hydrogels for cardiac tissue engineering. Macromol Biosci 18(6):1–22

Radisic M, Christman KL (2013) Materials science and tissue engineering: repairing the heart. Mayo Clin Proc 88(8):884–898

Rastogi RP, Kumar A, Tyagi MB, Sinha RP (2010) Molecular mechanisms of ultraviolet radiation-induced DNA damage and repair. J Nucleic Acids 2010:1–32

Severs NJ, Coppen SR, Dupont E, Yeh HI, Ko YS, Matsushita T (2004) Gap junction alterations in human cardiac disease. Cardiovasc Res 62(2):368–377

Severs NJ, Bruce AF, Dupont E, Rothery S (2008) Remodelling of gap junctions and connexin expression in diseased myocardium. Cardiovasc Res 80(1):9–19

Shevach M, Fleischer S, Shapira A, Dvir T (2014) Gold nanoparticle-decellularized matrix hybrids for cardiac tissue engineering. Nano Lett 14(10):5792–5796

Shin SR, Jung SM, Zalabany M, Kim K, Zorlutuna P, Kim SB, Nikkhah M, Khabiry M, Azize M, Kong J, Wan KT, Palacios T, Dokmeci MR, Bae H, Tang X, Khademhosseini A (2013) Carbon-nanotube-embedded hydrogel sheets for engineering cardiac constructs and bioactuators. ACS Nano 7(3):2369–2380

Tandon N, Cannizzaro C, Chao PHG, Maidhof R, Marsano A, Au HTH, Radisic M, Vunjak-Novakovic G (2009) Electrical stimulation systems for cardiac tissue engineering. Nat Protoc 4(2):155–173

Tous E, Purcell B, Ifkovits JL, Burdick JA (2011) Injectable acellular hydrogels for cardiac repair. J Cardiovasc Transl Res 4(5):528–542

Vunjak-Novakovic G, Tandon N, Godier A, Maidhof R, Marsano A, Martens TP, Radisic M (2010) Challenges in cardiac tissue engineering. Tissue Eng Part B 16(2):169–187

Wu Y, Li Y, Liu P, Gardner S, Ong BS (2006) Studies of gold nanoparticles as precursors to printed conductive features for thin-film transistors. Chem Mater 18(19):4627–4632